Peroxisome proliferator-activated receptor-α reduces inflammation and vascular leakage in a murine model of acute lung injury

M.B. Schaefer, A. Pose, J. Ott, M. Hecker, A. Behnk, R. Schulz, N. Weissmann, A. Günther, W. Seeger and K. Mayer

ABSTRACT: Acute lung injury (ALI) still represents a major cause of morbidity and mortality in intensive care units. Beneficial effects have been described after activation of the peroxisome proliferator-activated receptor (PPAR)-α by fibrates such as WY 14,643 (WY) in inflammatory models. In the present study, the impact of WY was investigated in a model of endotoxin (lipopolysaccharide; LPS)-induced ALI in mice.

Intratracheal LPS challenge dose-dependently resulted in leukocyte invasion, protein leakage and release of tumour necrosis factor-α as well as macrophage inflammatory protein-2, prostaglandin E_2 and thromboxane B_2 into the alveolar space after 8 and 24 h. Lung ventilator compliance was reduced at both time-points. In isolated perfused mouse lungs, platelet-activating factor (PAF) induced an acute increase in pulmonary artery pressure (Ppa) and in capillary filtration coefficient (Kfc). WY significantly improved all features of ALI *in vivo* and blunted the increase in Kfc in isolated perfused mice lungs. In mice with genetic deletion of PPAR-α, all characteristics of ALI, Ppa, and Kfc were not significantly different from wild-type mice but WY failed to improve ALI and PAF-induced increase in Kfc.

Activation of peroxisome proliferator-activated receptor-α by WY 14,643 reduced acute lung injury and vascular leakage. Fibrates may possess beneficial effects in acute pulmonary diseases beyond their lipid-lowering capability.

KEYWORDS: Acute lung injury, inflammation, peroxisome proliferator-activated receptor-α, vascular leakage

Acute respiratory distress syndrome (ARDS) and acute lung injury (ALI) are common clinical disorders characterised by alveolar epithelial and endothelial injury leading to the development of a protein-rich pulmonary oedema, elevation of pulmonary artery pressure (Ppa) and finally acute respiratory failure. According to recent data, the incidence of ALI or ARDS was 4.5–7.1% of all patients admitted to an intensive care unit (ICU), increasing to 12.5% when considering only patients treated for >24 h in the ICU [1, 2]. The high mortality rate associated with ARDS and ALI has declined to 30–40% in recent randomised trials [3] but still there is no proven pharmacological treatment, despite a multitude of strategies being successful in animal models [4]. Pathophysiological features of ALI include a compromised endothelial–alveolar barrier, leading to increased vascular permeability mirrored by the capillary filtration coefficient (Kfc), neutrophil migration into the lung tissue, and formation of pro-inflammatory mediators such as cytokines and eicosanoids (*e.g.* thromboxane (Tx)B_2 and prostaglandin (PG)E_2) [5].

Peroxisome proliferator-activated receptors (PPARs) are members of the nuclear hormone receptor superfamily of ligand-activated transcription factors, which are related to retinoid, steroid and thyroid hormone receptors [6]. The PPAR subfamily comprises three members: PPAR-α, PPAR-β/δ and PPAR-γ [7]. The name PPAR is derived from the fact that activation of PPAR-α by xenobiotics results in peroxisome proliferation in rodent hepatocytes. PPAR-α is highly expressed in brown adipose tissue, and to a lesser extent by liver, kidney, heart and skeletal muscle [8]. PPAR-α mRNA has been detected in murine lung tissue [9]. It has also been found in human endothelial cells,

as well as in smooth muscle cells, monocytes/macrophages and T-lymphocytes [10–12]. A diverse set of ligands binds to PPAR-α, such as arachidonic acid metabolites and synthetic fibrate drugs, including WY 14,643 (WY), clofibrate, fenofibrate and bezafibrate [13, 14]. Although PPAR-α has been less studied than PPAR-γ, PPAR-α ligands have also been shown to regulate inflammatory responses [15]. In addition, it has been demonstrated that PPAR-α-deficient mice have abnormally prolonged responses to different inflammatory stimuli [16–18]. Fibrates have exhibited anti-inflammatory properties *in vitro* [19, 20] as well as *in vivo* [15, 21]. In particular, it has been reported that PPAR-α ligands can inhibit the expression of various pro-inflammatory genes, such as interleukin (IL)-6, vascular cell adhesion molecule-1, platelet-activating factor (PAF) receptor and cyclooxygenase (COX)-2 (generating PGE_2 and TxB_2), in response to cytokine activation [21, 22]. This may, in part, be dependent on the inhibition of functional nuclear factor (NF)-κB activation and on the increase of expression of the inhibitory protein IκBα [23, 24]. The present study was carried out in order to gain a better understanding of the possible influence of PPAR-α in a mouse model of ALI.

MATERIALS AND METHODS

Reagents
Chemicals of the highest purity were obtained from Merck (Darmstadt, Germany). Lipopolysaccharide (LPS) from *E. coli* strain O111:B4, and WY, were from Sigma-Aldrich (Dreisenhofen, Germany).

Animals
The present study was approved by local government authorities (Giessen, Germany) and university officials responsible for animal protection (Justus-Liebig-University Giessen, Giessen). Parent and offspring PPAR-$\alpha^{-/-}$ and wild-type (WT) mice on the Sv129 background were kept under standard conditions with a 12-h day/night cycle under specific pathogen-free conditions. Animals 8–12 weeks old (18–21 g weight) were used for experiments. For intratracheal LPS instillation and measurement of compliance, mice were anaesthetised as described previously [25].

Determination of lung compliance by ventilator
When properly anaesthetised, mice were tracheotomised and ventilated in a volume-driven mode at a positive end-expiratory pressure of 0 kPa as described previously [26]. The respiration rate was set at 20 breaths·min^{-1} and ventilation pressure was recorded while inflating the lung at a tidal volume of 200 μL. The ventilator compliance is given and was corrected for animal weight.

Murine model of ALI
Mice were anaesthetised, a small catheter was inserted in the trachea, and LPS (1 or 10 μg in 50 μL normal saline per mouse) was instilled into the lung as described previously [25]. The mice were sacrificed 8 or 24 h after LPS application, and bronchoalveolar lavage (BAL) was performed [25]. Alveolar recruited leukocytes recovered from the lungs of LPS-challenged and control mice were counted using a counting chamber. Differentiation of leukocytes was performed in a blinded fashion using differential cell counts of Pappenheim-stained cytocentrifuge preparations, by overall morphological criteria, including differences in cell size and shape of nuclei.

Protein in BAL was determined according to the method of LOWRY *et al.* [27].

Isolated perfused and ventilated lung model
For determination of K_{fc} and haemodynamic measurements, a ventilated and perfused mouse lung preparation was used as previously described [28]. Briefly, mice were deeply anaesthetised and anticoagulated. After intubation *via* a tracheostoma, the mice were ventilated with a 250 μL tidal volume, 90 breaths·min^{-1} and 2 cmH$_2$O (0.2 kPa) positive end-expiratory pressure. Following midsternal thoracotomy, catheters were inserted into the pulmonary artery and left atrium. Sterilised perfusion circuit tubing was used throughout. Perfusion was performed using a peristaltic pump and Krebs-Henseleit buffer, containing 120 mM NaCl, 4.3 mM KCl, 1.1 mM KH$_2$PO$_4$, 2.4 mM CaCl$_2$, 1.3 mM MgCl$_2$ and 13.32 mM glucose, as well as 5% (weight/volume) hydroxyethylamylopectin (molecular weight 200 kDa). The pH was adjusted to 7.37–7.40 with NaHCO$_3$. After rinsing the lungs, the perfusion circuit was closed for recirculation and the left atrial pressure was set at 2.0 mmHg. Under steady-state conditions, perfusion flow was 2 mL·min^{-1}. Ppa and left atrial pressure were registered continuously *via* small-diameter catheters. The lungs were removed from the thorax and were placed in a temperature-equilibrated, humidified chamber at 37.0°C, freely suspended from a force transducer for monitoring of organ weight. The K_{fc} and the total vascular compliance were determined gravimetrically from the slope of the lung weight gain curve induced by a 7.5 mmHg-step elevation of the venous pressure for 8 min, as previously described [29].

Enzyme-linked immunosorbent assay
Tumour necrosis factor (TNF)-α, macrophage inflammatory protein (MIP)-2, PGE_2 and TxB_2 from BAL were determined by ELISA according to the manufacturer's instructions.

Experimental protocol
WY was given orally to WT and PPAR-$\alpha^{-/-}$ mice for 14 days at a dose of 1 mg·day^{-1}. This dose was chosen after performing pilot experiments with 0.5, 1 and 2 mg WY and determination of an upregulation of PPAR-α-dependent genes (*e.g.* fatty acid binding protein and lipoprotein lipase) in lung and liver homogenates by PCR, liver weight and bromodeoxyuridine staining in liver histology.

BAL for cytokine measurements (4–8 samples), protein determination (4–8 samples) and cell counts (4–8 samples), and lung compliance measurements (5–6 samples) were performed 8 or 24 h after intratracheal LPS instillation (0, 1 or 10 μg). In the isolated lung, after a steady-state period of 30 min, K_{fc} was determined (5–6 samples). PAF was injected into the pulmonary artery at 100 nmol·L^{-1} final concentration. Determination of K_{fc} was repeated 30 and 60 min after injection.

Statistics
Data are presented as mean±SEM. Two-way ANOVA was performed to test for differences between treatment groups (WT±WY, PPAR-$\alpha^{-/-}$±WY) and LPS dose (0, 1 and 10 μg) at each time-point. Repeated measures two-way ANOVA was used in the case of K_{fc} to detect differences between treatment groups (WT±WY, PPAR-$\alpha^{-/-}$±WY) and different time-points. *Post hoc* analysis was carried out using the Student-Newman-Keuls test. As the values for leukocytes, TNF-α, TxB_2 and PGE_2

were not normally distributed, log transformation was performed. Values of p<0.05 were considered statistically significant.

RESULTS

PPAR-α and alveolar transmigration of leukocytes in LPS-induced ALI

Without LPS, $0.24 \pm 0.05 \times 10^6$ leukocytes were recovered from BAL in WT mice. Comparable numbers were found after WY feeding and in PPAR-$\alpha^{-/-}$ mice, irrespective of WY treatment (fig. 1). The number of leukocytes in BAL increased to $0.81 \pm 0.06 \times 10^6$ and $0.96 \pm 0.13 \times 10^6$ 8 h after intratracheal instillation of 1 and 10 µg LPS, respectively. This increase in LPS-challenged mice was virtually the same in all groups examined (with or without WY, in WT and PPAR-$\alpha^{-/-}$ mice; p<0.05 versus respective baseline groups).

Leukocyte numbers in BAL increased further after 24 h to $1.49 \pm 0.18 \times 10^6$ and $2.12 \pm 0.13 \times 10^6$ in WT mice stimulated with 1 and 10 µg LPS, respectively. The rise in leukocyte numbers was significant in all groups receiving LPS, compared with the respective baseline groups (p<0.05). Similar numbers were detected in PPAR-$\alpha^{-/-}$ mice irrespective of WY treatment. In WT mice treated with WY, transmigration of leukocytes in the alveolar space was significantly reduced. After WY application and stimulation with 1 µg LPS, leukocytes decreased to 50% compared with WT mice not treated with WY, differing significantly from all other groups receiving this dose at this time-point (p<0.05; fig. 1). After challenge with 10 µg LPS, the WT+WY group exhibited a 33% reduction in leukocyte transmigration compared with WT mice, differing significantly from all other groups (p<0.05; fig. 1).

Without LPS challenge, the differential count of leukocytes in BAL in WT mice was $2.3 \pm 0.6\%$ granulocytes, $96.7 \pm 0.8\%$ monocytes/macrophages and $0.9 \pm 0.3\%$ lymphocytes. The distribution did not significantly differ from PPAR-$\alpha^{-/-}$ mice or from both groups receiving WY. In the BAL of WT mice, 24 h after challenge with 1 µg LPS, $75.3 \pm 2.9\%$ granulocytes, $22.7 \pm 3.0\%$ monocytes/macrophages and $1.9 \pm 0.3\%$ lymphocytes were detected. This profile of predominantly neutrophil invasion was not significantly changed in both PPAR-$\alpha^{-/-}$ groups or in WT mice with WY application. A similar distribution of leukocytes was detected in all groups receiving 10 µg LPS.

PPAR-α and TNF-α in LPS-induced ALI

The baseline TNF-α concentration in BAL of WT mice without LPS application was 49 ± 14 pg·mL^{-1} in control animals, and comparable concentrations were found in WT+WY as well as in both PPAR-$\alpha^{-/-}$ groups (fig. 2a and b). TNF-α in BAL rose to $1,262 \pm 126$ pg·mL^{-1} and $1,587 \pm 33$ pg·mL^{-1} 8 h after intratracheal instillation of 1 and 10 µg LPS in WT mice, respectively. This increase in LPS-challenged mice was nearly the same in all groups examined (p<0.01 versus baseline).

The concentration of TNF-α in BAL dropped after 24 h to 416 ± 45 pg·mL^{-1} and 534 ± 87 pg·mL^{-1} in WT mice stimulated with 1 and 10 µg LPS, respectively. Similar concentrations were measured in PPAR-$\alpha^{-/-}$ mice irrespective of WY treatment after application of 1 µg LPS. In both PPAR-$\alpha^{-/-}$ groups challenged with 10 µg LPS, TNF-α was slightly but not
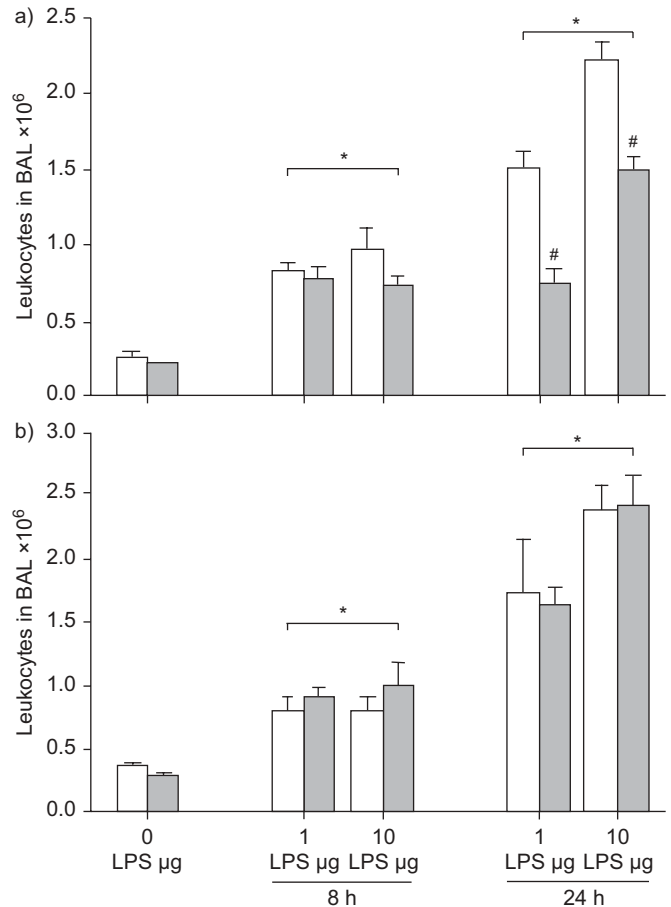

FIGURE 1. Peroxisome proliferator-activated receptor (PPAR)-α activation and leukocytes in bronchoalveolar lavage (BAL) in a model of acute lung injury. Wild-type (WT; a) and PPAR-$\alpha^{-/-}$ (b) mice were fed a diet enriched in WY 14,643 (WY; ■) or regular chow (□). Leukocytes were recovered from BAL at baseline (0 h), 8 h and 24 h after 1 or 10 µg intratracheal lipopolysaccharide (LPS) application. Leukocyte numbers increased after LPS stimulation, with all groups differing from their respective baseline. The rise in leukocyte numbers was reduced after WY pretreatment in WT mice compared with all other groups receiving the same dose. Data are presented as mean ± SEM, 4–8 independent experiments each. Error lines are missing when contained within bar. #: p<0.05 for WT+WY after LPS applications compared with other groups receiving the same LPS dose. *: p<0.05 for groups exposed to LPS versus respective baseline.

significantly higher compared with WT mice without WY treatment. All groups receiving LPS differed significantly from their baseline groups (p<0.01). WT mice treated with WY exhibited a reduction in TNF-α concentration to 33% and 59% after 1 and 10 µg LPS application, respectively. Both WT+WY groups differed significantly from all other groups receiving the same dose of LPS (1 µg: p<0.01; 10 µg: p<0.05) and from their respective baseline groups (1 µg: p<0.05; 10 µg: p<0.01).

PPAR-α and MIP-2 in LPS-induced ALI

The baseline MIP-2 concentration in BAL of WT mice without LPS application was 150 ± 53 pg·mL^{-1} in control animals and 115 ± 16 pg·mL^{-1} in WY-treated mice (fig. 2c). In PPAR-$\alpha^{-/-}$ mice (fig. 2d), MIP-2 was slightly but not significantly higher
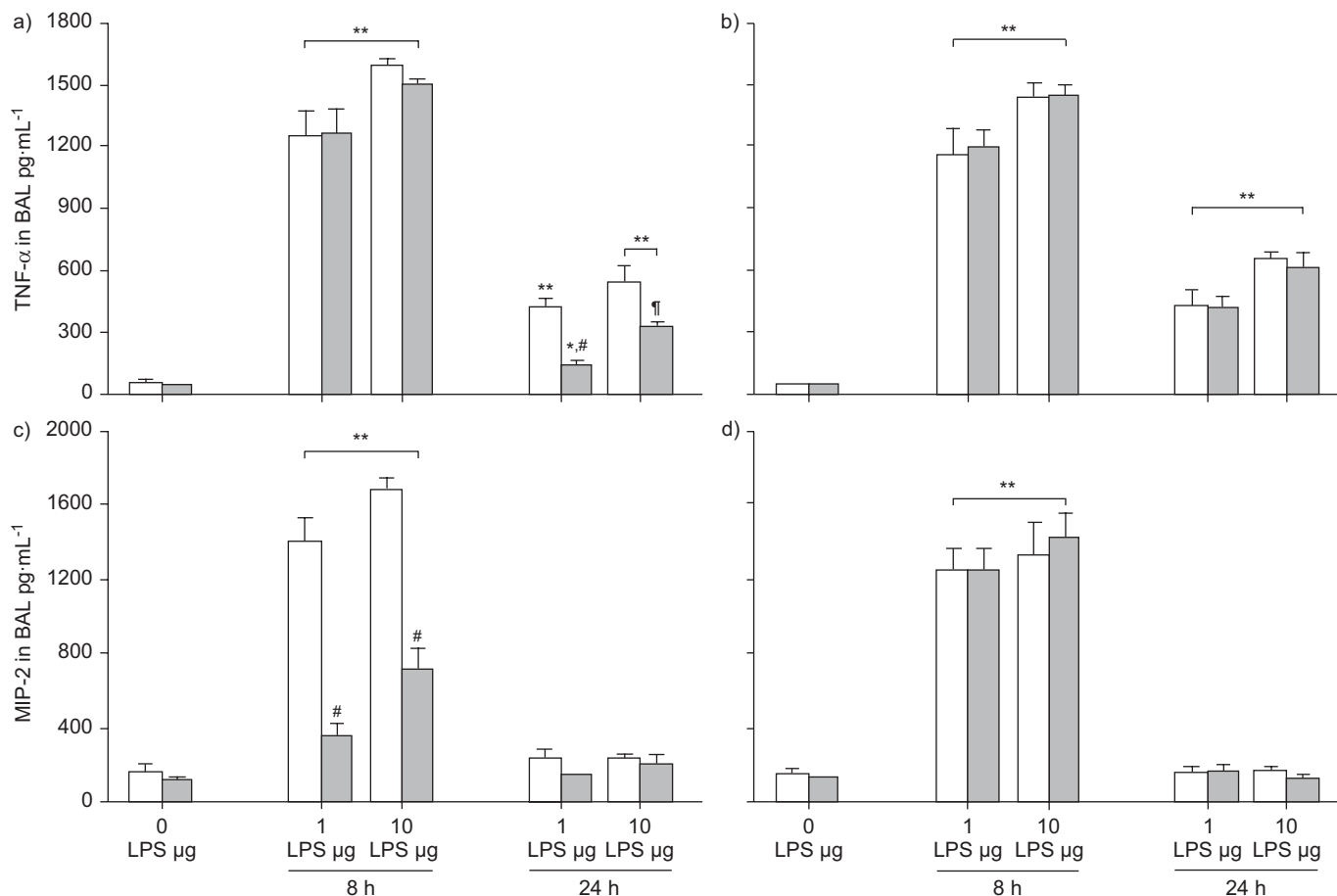
FIGURE 2. Peroxisome proliferator-activated receptor (PPAR)-α activation and cytokine generation in bronchoalveolar lavage (BAL) in a model of acute lung injury. Wild-type (WT; a and c) and PPAR-α$^{-/-}$ (b and d) mice were fed a diet enriched in WY 14,643 (WY; ■) or regular chow (□). Tumour necrosis factor (TNF)-α (a and b) and macrophage inflammatory protein (MIP)-2 (c and d) concentrations were determined in BAL at baseline (0 h), 8 h and 24 h after 1 or 10 μg intratracheal lipopolysaccharide (LPS) application. TNF-α was significantly different for all groups exposed to LPS *versus* respective baseline. MIP-2 rose significantly after LPS exposure, with all LPS-treated groups differing from their baseline. Concentrations of TNF-α and MIP-2 in WT+WY after LPS applications were significantly lower compared with all other groups receiving the same dose. Data are presented as mean ± SEM, 4–8 independent experiments each. Error lines are missing when contained within bar. $^{\#}$: p<0.01; ¶: p<0.05 for WT+WY after LPS applications compared with other groups receiving the same LPS dose. *: p<0.05; **: p<0.01 for groups exposed to LPS *versus* respective baseline.

compared with WT animals. MIP-2 in BAL rose to 1,400±120 pg·mL^{-1} and 1,681±57 pg·mL^{-1} 8 h after intratracheal instillation of 1 and 10 μg LPS in WT mice, respectively. All groups receiving LPS differed significantly from baseline (p<0.01). MIP-2 was slightly but not significantly higher in PPAR-α$^{-/-}$ mice challenged with 1 μg LPS and comparable to WT mice after application of 10 μg LPS. Treatment with WY reduced the rise in MIP-2 to 26% or 42% in WT mice after challenge with 1 or 10 μg LPS, respectively. WT mice receiving WY differed significantly from all other groups with the same LPS dose (p<0.01 for both doses; fig. 2c).

After 24 h, the concentration of MIP-2 in BAL dropped to 232±44 pg·mL^{-1} and 231±18 pg·mL^{-1} in WT mice receiving 1 and 10 μg LPS, respectively. All other groups (WT+WY, PPAR-α$^{-/-}$±WY) also returned to baseline and no significant difference was observed.

PPAR-α and lung compliance in LPS-induced ALI
Baseline lung compliance in WT mice without LPS application was 5.27±0.29 L·kPa^{-1}·kg^{-1} in control animals and there was

no significant variation in all other groups at baseline (fig. 3). Compliance was markedly reduced in WT mice 8 h after intratracheal challenge with 1 and 10 μg LPS (4.02±0.12 and 3.43±0.17 L·kPa^{-1}·kg^{-1}, respectively), with PPAR$^{-/-}$±WY exhibiting similar values (p<0.05 *versus* baseline). In WT mice receiving WY, compliance remained higher and animals receiving 10 μg LPS differed from all other groups with that dose of LPS (p<0.05).

After 24 h, compliance was further reduced in WT animals and both PPAR-α$^{-/-}$ groups (p<0.05 *versus* baseline). In contrast, an improvement in lung compliance was found in WT animals receiving WY (p<0.05 *versus* all other groups receiving 1 μg LPS at 24 h).

PPAR-α and protein concentration in LPS-induced ALI
Before LPS challenge, protein concentration in BAL was 0.21±0.03 μg·mL^{-1}, with no significant differences due to strain or WY treatment (fig. 4a and b). Protein concentration increased to nearly 400% of baseline 8 h after 1 μg LPS instillation in WT mice as well as in both PPAR-α$^{-/-}$ groups (p<0.05 *versus* baseline).
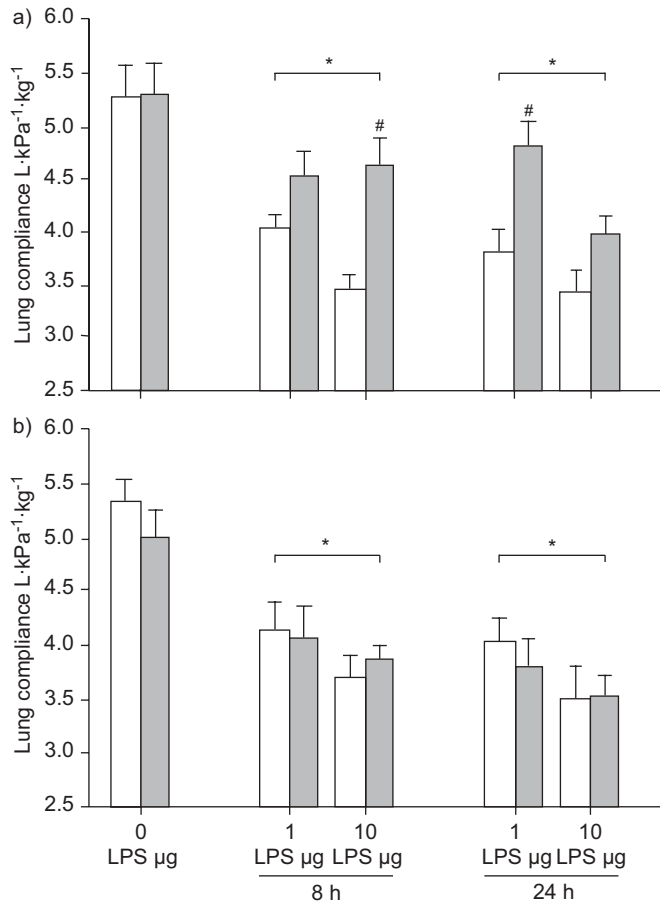
FIGURE 3. Peroxisome proliferator-activated receptor (PPAR)-α activation and lung compliance in a model of acute lung injury. Wild-type (WT; a) and PPAR-α$^{-/-}$ (b) mice were fed a diet enriched in WY 14,643 (WY; ■) or regular chow (□). Lung compliance was determined at baseline (0 h), 8 h and 24 h after 1 or 10 μg intratracheal lipopolysaccharide (LPS) application. Lung compliance was decreased after LPS instillation in WT mice and both PPAR-α$^{-/-}$ groups compared with baseline. WT mice receiving WY exhibited protection against loss of compliance after 10 μg LPS at 8 h and after 1 μg LPS at 24 h compared with all other groups at the respective time-points. Data are presented as mean±SEM, 5–6 independent experiments each. $^{#}$: p<0.05 for WT+WY after LPS applications compared with other groups receiving the same LPS dose. *: p<0.05 for groups exposed to LPS versus respective baseline.

In WT mice receiving WY, the increase was markedly blunted and the protein concentration rose only to 0.45 ± 0.06 μg·mL^{-1} (p<0.05 versus all other groups receiving 1 μg LPS and versus baseline). Protein concentration was further increased in WT animals after instillation of 10 μg LPS after 8 h, with similar values determined in both PPAR-α$^{-/-}$ groups (p<0.05 versus baseline). Again, a marked reduction by nearly 50% was found in WT mice after WY treatment (p<0.05 versus all other groups receiving 10 μg LPS and versus baseline). After 24 h, protein concentrations in animals receiving 1 or 10 μg LPS were slightly lower compared with corresponding groups at 8 h. However, at this time-point, the differences were not statistically significant.

PPAR-α and K_{fc} in isolated perfused lungs

To examine whether the increased BAL protein concentration would be mirrored by a reduction in endothelial barrier function, K_{fc} was measured in a murine isolated perfused lung model. Lungs were isolated from WT and PPAR-α$^{-/-}$ mice without LPS challenge and 8 or 24 h after LPS instillation. However, the current authors were not able to obtain stable baseline conditions at any time after LPS challenge. Therefore, only the data from mice prior to LPS challenge, with PAF as acute stimulus, are reported in the isolated perfused lung model. Baseline K_{fc} was similar in all groups (fig. 4c). Challenge with PAF resulted in an acute increase in P_{pa} by 5.1 mmHg with no significant difference between the groups (data not shown). After 30 min, K_{fc} was nearly tripled in WT mice and in PPAR-α$^{-/-}$ mice irrespective of WY treatment. WT animals pretreated with WY exhibited a blunted increase in K_{fc} (p<0.01 versus all other groups at 30 min). K_{fc} returned to baseline values 60 min after PAF challenge. The increase in K_{fc} directly after PAF challenge was significant compared with baseline as well as with the determination after 60 min (p<0.01 for all groups apart from WT+WY).

PPAR-α and TxB_2 in LPS-induced ALI

Before LPS challenge, the concentration of TxB_2 in BAL was 214 ± 27 pg·mL^{-1}, with no significant differences due to strain or WY treatment (fig. 5a and b). After 8 h, the concentrations of TxB_2 increased to 471 ± 36 pg·mL^{-1} and 535 ± 54 pg·mL^{-1} in WT mice challenged with 1 or 10 μg LPS, respectively. The rise in TxB_2, irrespective of LPS dose, was significant for these three groups (WT, PPAR-α$^{-/-}$ with WY and PPAR-α$^{-/-}$ without WY) compared with baseline (p<0.05). WT mice receiving WY showed a blunted increase in TxB_2 concentrations after 1 and 10 μg LPS of nearly 20% or nearly 30%, respectively, which reached a significant level only after challenge with 10 μg LPS (p<0.05 versus all other groups receiving the same dose). The increase in TxB_2 after LPS in these mice was not significant compared with baseline.

After 24 h, 466 ± 54 pg·mL^{-1} and 599 ± 78 pg·mL^{-1} TxB_2 were measured in WT mice receiving 1 and 10 μg LPS, respectively (fig. 5a). Similar concentrations were detected in corresponding PPAR-α$^{-/-}$ groups, irrespective of WY application (fig. 5b). All groups differed from their respective baseline (p<0.05). WT mice with WY pretreatment exhibited a marked reduction in TxB_2 concentration at this time-point, reaching a significant level in mice receiving 10 μg LPS (p<0.05 versus all other groups receiving this dose; fig. 5a and b). The increase in TxB_2 after LPS application was not significant compared with baseline in both groups.

PPAR-α and PGE_2 in LPS-induced ALI

Before LPS instillation, the concentration of PGE_2 in BAL was 296 ± 28 pg·mL^{-1}, with similar values measured in both PPAR-α$^{-/-}$ groups (fig. 5c and d). PGE_2 was lower in WT mice receiving WY, but the difference was not statistically significant. In WT mice, 8 h after LPS challenge, PGE_2 rose to 873 ± 127 pg·mL^{-1} and $2,048 \pm 185$ pg·mL^{-1} in mice challenged with 1 and 10 μg LPS, respectively. The PGE_2 concentration was significantly different from baseline in all groups after both doses of LPS (p<0.05). Concentrations found in all PPAR-α$^{-/-}$ groups at this time-point did not differ significantly from WT mice. However, in WT mice receiving WY, the rise in PGE_2 was blunted to 601 ± 31 pg·mL^{-1} and 723 ± 35 pg·mL^{-1} (p<0.05 versus all other groups) after 1 and 10 μg LPS,
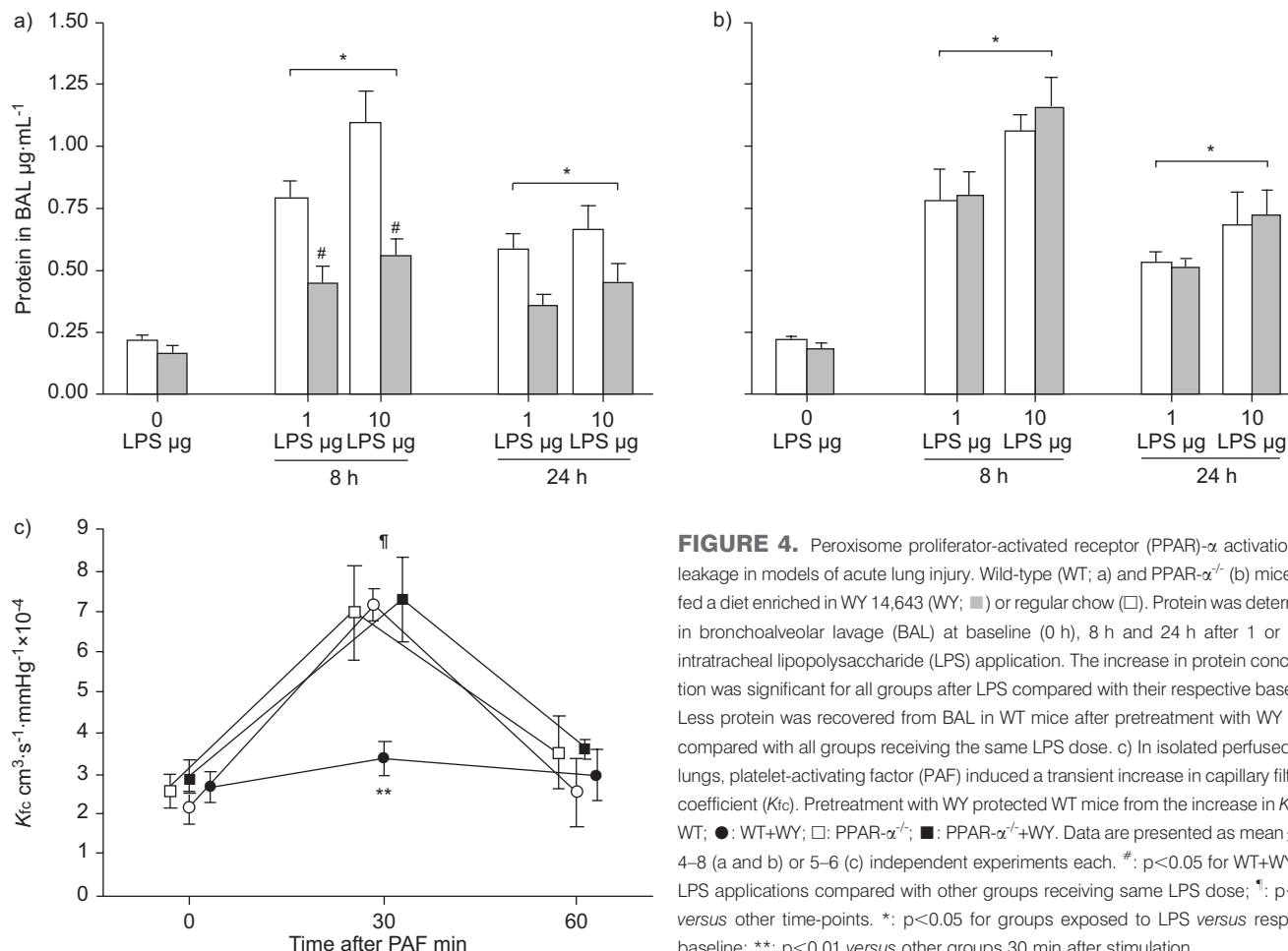
FIGURE 4. Peroxisome proliferator-activated receptor (PPAR)-α activation and leakage in models of acute lung injury. Wild-type (WT; a) and PPAR-$\alpha^{-/-}$ (b) mice were fed a diet enriched in WY 14,643 (WY; ■) or regular chow (□). Protein was determined in bronchoalveolar lavage (BAL) at baseline (0 h), 8 h and 24 h after 1 or 10 µg intratracheal lipopolysaccharide (LPS) application. The increase in protein concentration was significant for all groups after LPS compared with their respective baselines. Less protein was recovered from BAL in WT mice after pretreatment with WY at 8 h compared with all groups receiving the same LPS dose. c) In isolated perfused mice lungs, platelet-activating factor (PAF) induced a transient increase in capillary filtration coefficient (Kfc). Pretreatment with WY protected WT mice from the increase in Kfc. ○: WT; ●: WT+WY; □: PPAR-$\alpha^{-/-}$; ■: PPAR-$\alpha^{-/-}$+WY. Data are presented as mean ± SEM, 4–8 (a and b) or 5–6 (c) independent experiments each. #: $p < 0.05$ for WT+WY after LPS applications compared with other groups receiving same LPS dose; ¶: $p < 0.01$ versus other time-points. *: $p < 0.05$ for groups exposed to LPS versus respective baseline; **: $p < 0.01$ versus other groups 30 min after stimulation.

respectively. The difference in PGE_2 after 1 and 10 µg LPS was significant ($p < 0.05$) in all groups except in WT mice after treatment with WY.

PGE_2 rose further after 24 h to $1,172 \pm 107$ pg·mL^{-1} and $2,460 \pm 158$ pg·mL^{-1} in WT mice receiving 1 µg and 10 µg LPS, respectively (fig. 5c). No significant difference from the respective PPAR-$\alpha^{-/-}$ groups was found (fig. 5d). In contrast, PGE_2 was reduced to ~60% irrespective of LPS challenge in WT mice after feeding with WY. The difference was significant compared with all corresponding groups receiving the same LPS dose ($p < 0.05$). PGE_2 concentrations differed significantly from baseline after both LPS challenges in all groups ($p < 0.05$). Again, a dose-dependent increase in PGE_2 was found, with concentrations after challenge with 1 µg LPS being significantly lower compared with those after 10 µg LPS in all groups ($p < 0.05$).

DISCUSSION

In the present study, it was demonstrated that activation of the transcription factor PPAR-α by the fibrate WY is protective in a murine model of ALI in vivo and in PAF-induced increase in vascular leakage in isolated perfused mice lungs. WY was able to reduce LPS-provoked invasion of neutrophils into the alveolar space and generation of inflammatory mediators such as TNF-α, MIP-2, TxB_2 and PGE_2. Furthermore, integrity of the endothelial–alveolar barrier was preserved by treatment with

WY, as judged by decreased protein concentration in the BAL and a reduced Kfc. As an additional functional parameter, WY reduced acute deterioration of lung compliance in LPS-challenged mice. In PPAR-α-deficient mice, treatment with WY did not evoke these beneficial changes in ALI either in vivo or in isolated perfused mice lungs. However, it should be kept in mind that a drawback of the LPS model is the use of endotoxin in a single-hit model to induce inflammatory responses. Such a model is clearly different from ARDS or ALI due to prolonged bacterial infection.

Expression of PPAR-α is high in liver, kidney, muscle and heart [30], but has also been detected in smooth muscle cells, monocytes/macrophages and T-lymphocytes [10]. PPAR-α-dependent genes regulate metabolism of fatty acids and lipoproteins but evidence is accumulating that fibrates activating PPAR-α not only possess lipid-lowering properties but are also exerting beneficial actions in pulmonary diseases [10]. Most authors describe positive effects of PPAR-α activation in prolonged models of pulmonary diseases but an impact in per-acute lung injury (not focusing on airway or pleural inflammation) was lacking. Protection from the inflammatory response by a PPAR-α ligand was found in a prolonged (15 days) murine lung injury model induced by bleomycin [31]. Activation of PPAR-α by WY induced a reduction of the bleomycin-induced increases in TNF-α, IL-1, poly-ADP-ribose and mortality. In contrast, loss of the
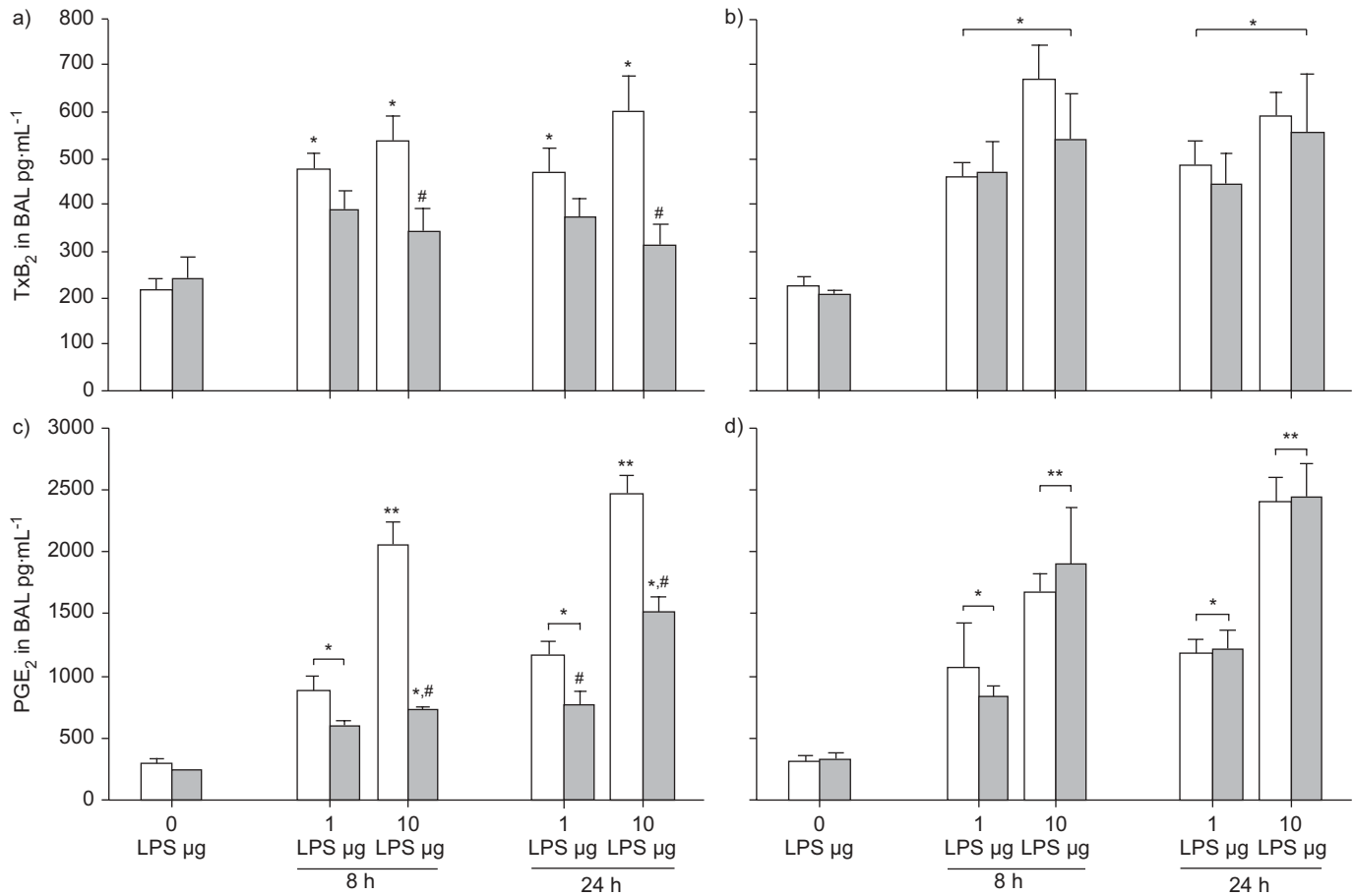
FIGURE 5. Peroxisome proliferator-activated receptor (PPAR)-α activation and prostanoid generation in bronchoalveolar lavage (BAL) in a model of acute lung injury. Wild-type (WT; a and c) and PPAR-α$^{-/-}$ (b and d) mice were fed a diet enriched in WY 14,643 (WY; ■) or regular chow (□). Thromboxane (Tx)B$_2$ (a and b) or prostaglandin (PG)E$_2$ (c and d) were determined in BAL at baseline (0 h), 8 h and 24 h after 1 or 10 μg intratracheal lipopolysaccharide (LPS) application. After challenge with 1 and 10 μg LPS, TxB$_2$ increased in all groups except WT mice receiving WY. The WT+WY group differed from all other groups after 10 μg LPS. PGE$_2$ also rose after LPS challenge, with all groups differing from their respective baseline. Compared with all other groups receiving the same LPS dose, PGE$_2$ concentrations were significantly lower in WT+WY mice after 10 μg LPS (at 8 h and 24 h) and after 1 μg LPS (at 24 h). Data are presented as mean±SEM, 4–8 independent experiments each. Error lines are missing when contained within bar. $^{#}$: p<0.05 for WT+WY after LPS applications compared with other groups receiving the same LPS dose. *: p<0.05; **: p<0.01 for groups exposed to LPS *versus* respective baseline.

functional PPAR-α pathway in PPAR-α$^{-/-}$ mice increased all reported parameters [31]. In a model of carrageen-induced pleurisy, PPAR-α$^{-/-}$ mice showed increased generation of TNF-α, IL-1 and FAS-ligand, and increased leukocyte infiltration [32]. In a model of prolonged airway inflammation induced by chronic intranasal LPS challenge, leukocyte infiltration, TNF-α, monocyte chemoattractant protein-1, keratinocyte-derived chemokine and matrix metalloproteinases were increased after 5 days in mice lacking functional PPAR-α receptor. In contrast, treatment with fenofibrate reduced all examined parameters [33]. In line with these findings, allergic airway inflammation was reduced by fenofibrate in ovalbumin-sensitised mice [34]. It has been demonstrated that activation of PPAR-α interferes with the expression of pro-inflammatory genes such as vascular cell adhesion molecule (VCAM)-1, PAF receptor and COX-2 [21, 22]. This may be mediated at least partly by reduced activation of NF-κB and increased expression of its inhibitor IκBα [23, 24]. Both effects may result in a decreased nuclear translocation of p50/p65 NF-κB after

inflammatory stimulation, thereby affecting nuclear transcription of dependent genes such as TNF-α and IL-1. As down-stream effects of LPS are mediated at least in part by activation of NF-κB, inhibition of this pathway may also be responsible for the reduction of ALI. The present data, showing reduced generation of TNF-α, MIP-2, TxB$_2$ and PGE$_2$ after LPS challenge in mice, are consistent with this analysis.

However, this reasoning may not fully explain the beneficial effects of WY on pulmonary permeability. In murine lungs, PAF induced an acute increase in vasoconstriction and permeability [35]. The acute vasoconstriction is mediated by generation of cysteinyl-leukotrienes and TxA$_2$ [35]. Immediate formation of PGE$_2$ by COX-1 and activation of the acid sphingomyelinase (ASM) with subsequent synthesis of ceramides are the key events inducing permeability [36]. In isolated lungs, the current authors found an unchanged vasoconstriction, mirrored by the perfusion pressure, despite activation of PPAR-α by WY. In contrast, the PAF-induced

increase in K_{fc} (a marker of permeability) was nearly abolished. As both vasoconstriction and permeability involve receptor-dependent activation of secondary mediators, a downregulation of PAF receptors by PPAR-α agonists, as found in human macrophages [22], seems unlikely in the mice used in the present study. The current authors speculate that WY protected the lungs from PAF-induced permeability due inhibition of the PGE_2 (COX-1) or ceramide (ASM) pathway [36]. Evidence is accumulating that activation of PPAR-α induces an increase in ceramides, although these data were generated in hearts and not in lungs [37, 38]. Taking this together with the reduction in PGE_2 as determined in the BAL after LPS challenge *in vivo*, the COX-1 and COX-2 pathways can be considered primary targets of PPAR-α in effects on permeability in the present model.

As already discussed, activation of PPAR-α was reported to reduce inflammation in the lungs. Conversely, genetic deletion of PPAR-α induced prolonged and increased inflammation, as judged, for example, by increased generation of pro-inflammatory cytokines, leukocyte infiltration and mortality [31–34]. Whereas the data from the present ALI model are consistent with the first part of these findings, only a small (not significant) increase in the LPS-induced response was found in mice lacking functional PPAR-α and thus lacking responses from exogenous or endogenous activators. These diverging results may be due to the different time-points and models. While the present study used per-acute models of ALI, taking minutes in the isolated lung and 24 h *in vivo* as time period, the diverging results are derived from models that are more chronic and focus mainly on airway or pleural inflammation involving time spans of 5–14 days. In contrast, the present study confirmed that the beneficial effects of WY in pulmonary pathologies were specifically dependent on functional PPAR-α. Using PPAR-$\alpha^{-/-}$ mice, the protective effects of WY on cytokines, eicosanoids, leukocyte infiltration and vascular leakage in models of ALI were abolished. These findings are in line with previous studies using WY or fenofibrate [31–34]. TRIFILIEFF *et al.* [39] were unable to detect the same protective effects of the PPAR-α agonist GW 9578 in mice. However, they applied GW 9578 intranasally 1 h before LPS instillation and did not find reduced TNF-α generation in BAL or a change in neutrophil influx. A clue to the understanding of these diverging results may be the difference in the application of fibrates. The application of GW 9578 just 1 h before the inflammatory challenge may have been too short for the beneficial actions of PPAR-α activation, *e.g.* for subsequent changes in protein expression of NF-κB-dependent genes to take place. Next, TRIFILIEFF *et al.* [39] used a local (intranasal) application whereas other studies and the present study used a systemic approach: feeding the mice or using intraperitoneal injection. Despite expression of PPAR-α in murine lungs [9] and a direct impact of fibrates on airway smooth muscle cells [40], it is possible that local as well as remote leukocytes and endothelial cells must also be targeted for the full effect of fibrates to take place.

Leukocyte transmigration into the alveolar space represents a characteristic of pulmonary inflammation and ALI [41]. The present study showed that activation of PPAR-α reduced acute neutrophil invasion in the model of ALI. As neutrophil transmigration into the alveolar space needs a concerted action of neutrophils, endothelial cells and epithelial cells, an impact of WY on all cell populations may be possible. A reduced expression of VCAM-1 in endothelial cells and PAF receptor in leukocytes has already been shown [21, 22], and both systems are involved in adhesion and transmigration of leukocytes [42]. Furthermore, reduced generation of MIP-2 (the murine equivalent of the chemotaxin IL-8 in humans) as found in the present study and decreased TxA_2 synthesis represent two further causes of the reduced leukocyte infiltration in the lungs.

Finally, the present study provides evidence that LPS instillation into the lungs significantly impairs lung compliance. This impairment is ameliorated by WY-induced PPAR-α activation. Determination of compliance represents a recognised means to evaluate lung injury [43] and impairment is found in patients with ALI [44]. The fact that PPAR-α activation improved compliance underscores the beneficial effects of PPAR-α activation on ALI.

The beneficial impact of fibrates in the present ALI model is best described through the blunting and shortening of the ability of LPS to induce an inflammatory response. The invasion of leukocytes into the alveolar space was decreased 24 h after the initiation of the lung injury. This may be attributed to the reduced generation of MIP-2 at 8 h after LPS instillation, which, in addition to the decreased release of TxB_2 at both time-points, may be responsible for the lower influx of neutrophils. The impact of fibrates on TNF-α was only visible at the second time-point, as the generation of TNF-α was unchanged at 8 h but was decreased at 24 h after the injury. This is in contrast to the effect of fibrates on COX-derived PGE_2 and TxB_2, on protein in BAL and on compliance. All these variables were generally improved at both time-points after LPS instillation by application of fibrates. This feature adds to the idea that inhibition of COX may be a key player in translating the effects of fibrates in ALI.

In conclusion, the present study demonstrated that pretreatment with WY 14,643 reduced generation of pro-inflammatory cytokines and eicosanoids, blunted alveolar leukocyte invasion and improved compliance as well as vascular leakage in mice. The protective potency of WY 14,643 is dependent on functional peroxisome proliferator-activated receptor-α. Further investigations are warranted to explore the effect of fibrates in patients with inflammatory pulmonary pathologies.

REFERENCES
1 Brun-Buisson C, Minelli C, Bertolini G, *et al.* Epidemiology and outcome of acute lung injury in European intensive care units. Results from the ALIVE study. *Intensive Care Med* 2004; 30: 51–61.
2 Esteban A, Anzueto A, Frutos F, *et al.* Characteristics and outcomes in adult patients receiving mechanical ventilation: a 28-day international study. *JAMA* 2002; 287: 345–355.

3 Wheeler AP, Bernard GR. Acute lung injury and the acute respiratory distress syndrome: a clinical review. *Lancet* 2007; 369: 1553–1564.

4 Calfee CS, Matthay MA. Nonventilatory treatments for acute lung injury and ARDS. *Chest* 2007; 131: 913–920.

5 Matthay MA, Zimmerman GA. Acute lung injury and the acute respiratory distress syndrome: four decades of inquiry into pathogenesis and rational management. *Am J Respir Cell Mol Biol* 2005; 33: 319–327.

6 Evans RM. The steroid and thyroid hormone receptor superfamily. *Science* 1988; 240: 889–895.

7 Murphy GJ, Holder JC. PPAR-γ agonists: therapeutic role in diabetes, inflammation and cancer. *Trends Pharmacol Sci* 2000; 21: 469–474.

8 Cabrero A, Laguna JC, Vazquez M. Peroxisome proliferator-activated receptors and the control of inflammation. *Curr Drug Targets Inflamm Allergy* 2002; 1: 243–248.

9 Becker J, Delayre-Orthez C, Frossard N, Pons F. Regulation of peroxisome proliferator-activated receptor-α expression during lung inflammation. *Pulm Pharmacol Ther* 2008; 21: 324–330.

10 Paola RD, Cuzzocrea S. Peroxisome proliferator-activated receptors and acute lung injury. *PPAR Res* 2007; 2007: 63745.

11 Rival Y, Beneteau N, Taillandier T, *et al.* PPARα and PPARδ activators inhibit cytokine-induced nuclear translocation of NF-κB and expression of VCAM-1 in EAhy926 endothelial cells. *Eur J Pharmacol* 2002; 435: 143–151.

12 Marx N, Sukhova GK, Collins T, Libby P, Plutzky J. PPARα activators inhibit cytokine-induced vascular cell adhesion molecule-1 expression in human endothelial cells. *Circulation* 1999; 99: 3125–3131.

13 Sher T, Yi HF, McBride OW, Gonzalez FJ. cDNA cloning, chromosomal mapping, and functional characterization of the human peroxisome proliferator activated receptor. *Biochemistry* 1993; 32: 5598–5604.

14 Toyama T, Nakamura H, Harano Y, *et al.* PPARα ligands activate antioxidant enzymes and suppress hepatic fibrosis in rats. *Biochem Biophys Res Commun* 2004; 324: 697–704.

15 Lovett-Racke AE, Hussain RZ, Northrop S, *et al.* Peroxisome proliferator-activated receptor-α agonists as therapy for autoimmune disease. *J Immunol* 2004; 172: 5790–5798.

16 Devchand PR, Keller H, Peters JM, Vazquez M, Gonzalez FJ, Wahli W. The PPARα-leukotriene B$_4$ pathway to inflammation control. *Nature* 1996; 384: 39–43.

17 Staels B, Koenig W, Habib A, *et al.* Activation of human aortic smooth-muscle cells is inhibited by PPARα but not by PPARγ activators. *Nature* 1998; 393: 790–793.

18 Cuzzocrea S, Di Paola R, Mazzon E, *et al.* Role of endogenous and exogenous ligands for the peroxisome proliferators activated receptors α (PPAR-α) in the development of inflammatory bowel disease in mice. *Lab Invest* 2004; 84: 1643–1654.

19 Takano H, Nagai T, Asakawa M, *et al.* Peroxisome proliferator-activated receptor activators inhibit lipopolysaccharide-induced tumor necrosis factor-α expression in neonatal rat cardiac myocytes. *Circ Res* 2000; 87: 596–602.

20 Okamoto H, Iwamoto T, Kotake S, Momohara S, Yamanaka H, Kamatani N. Inhibition of NF-κB signaling

by fenofibrate, a peroxisome proliferator-activated receptor-α ligand, presents a therapeutic strategy for rheumatoid arthritis. *Clin Exp Rheumatol* 2005; 23: 323–330.

21 Delerive P, De Bosscher K, Besnard S, *et al.* Peroxisome proliferator-activated receptor-α negatively regulates the vascular inflammatory gene response by negative cross-talk with transcription factors NF-κB and AP-1. *J Biol Chem* 1999; 274: 32048–32054.

22 Hourton D, Delerive P, Stankova J, Staels B, Chapman MJ, Ninio E. Oxidized low-density lipoprotein and peroxisome-proliferator-activated receptor-α down-regulate platelet-activating-factor receptor expression in human macrophages. *Biochem J* 2001; 354: 225–232.

23 Delerive P, Gervois P, Fruchart JC, Staels B. Induction of IκBα expression as a mechanism contributing to the anti-inflammatory activities of peroxisome proliferator-activated receptor-α activators. *J Biol Chem* 2000; 275: 36703–36707.

24 Spencer NF, Poynter ME, Im SY, Daynes RA. Constitutive activation of NF-κB in an animal model of aging. *Int Immunol* 1997; 9: 1581–1588.

25 Schaefer MB, Ott J, Mohr A, *et al.* Immunomodulation by n-3- *versus* n-6-rich lipid emulsions in murine acute lung injury – role of platelet-activating factor receptor. *Crit Care Med* 2007; 35: 544–554.

26 Wygrecka M, Markart P, Ruppert C, *et al.* Cellular origin of pro-coagulant and (anti)-fibrinolytic factors in bleomycin-injured lungs. *Eur Respir J* 2007; 29: 1105–1114.

27 Lowry OH, Rosebrough NJ, Farr AL, Randall RJ. Protein measurement with the Folin phenol reagent. *J Biol Chem* 1951; 193: 265–275.

28 Weissmann N, Dietrich A, Fuchs B, *et al.* Classical transient receptor potential channel 6 (TRPC6) is essential for hypoxic pulmonary vasoconstriction and alveolar gas exchange. *Proc Natl Acad Sci USA* 2006; 103: 19093–19098.

29 Grimminger F, Wahn H, Mayer K, Kiss L, Walmrath D, Seeger W. Impact of arachidonic *versus* eicosapentaenoic acid on exotonin-induced lung vascular leakage: relation to 4-series *versus* 5-series leukotriene generation. *Am J Respir Crit Care Med* 1997; 155: 513–519.

30 Clark RB. The role of PPARs in inflammation and immunity. *J Leukoc Biol* 2002; 71: 388–400.

31 Genovese T, Mazzon E, Di Paola R, *et al.* Role of endogenous and exogenous ligands for the peroxisome proliferator-activated receptor-α in the development of bleomycin-induced lung injury. *Shock* 2005; 24: 547–555.

32 Cuzzocrea S, Mazzon E, Di Paola R, *et al.* The role of the peroxisome proliferator-activated receptor-α (PPAR-α) in the regulation of acute inflammation. *J Leukoc Biol* 2006; 79: 999–1010.

33 Delayre-Orthez C, Becker J, Guenon I, *et al.* PPARα downregulates airway inflammation induced by lipopolysaccharide in the mouse. *Respir Res* 2005; 6: 91.

34 Delayre-Orthez C, Becker J, Auwerx J, Frossard N, Pons F. Suppression of allergen-induced airway inflammation and immune response by the peroxisome proliferator-activated receptor-alpha agonist fenofibrate. *Eur J Pharmacol* 2008; 581: 177–184.

35 Uhlig S, Göggel R, Engel S. Mechanisms of platelet-activating factor (PAF)-mediated responses in the lung. *Pharmacol Rep* 2005: 57: Suppl., 206–221.

36 Göggel R, Winoto-Morbach S, Vielhaber G, *et al.* PAF-mediated pulmonary edema: a new role for acid sphingomyelinase and ceramide. *Nat Med* 2004; 10: 155–160.

37 Morgan EE, Rennison JH, Young ME, *et al.* Effects of chronic activation of peroxisome proliferator-activated receptor-α or high-fat feeding in a rat infarct model of heart failure. *Am J Physiol Heart Circ Physiol* 2006; 290: H1899–H1904.

38 Finck BN, Han X, Courtois M, *et al.* A critical role for PPARα-mediated lipotoxicity in the pathogenesis of diabetic cardiomyopathy: modulation by dietary fat content. *Proc Natl Acad Sci USA* 2003; 100: 1226–1231.

39 Trifilieff A, Bench A, Hanley M, Bayley D, Campbell E, Whittaker P. PPAR-α and -γ but not -δ agonists inhibit airway inflammation in a murine model of asthma: *in vitro* evidence for an NF-κB-independent effect. *Br J Pharmacol* 2003; 139: 163–171.

40 Patel HJ, Belvisi MG, Bishop-Bailey D, Yacoub MH, Mitchell JA. Activation of peroxisome proliferator-activated receptors in human airway smooth muscle cells has a superior anti-inflammatory profile to corticosteroids: relevance for chronic obstructive pulmonary disease therapy. *J Immunol* 2003; 170: 2663–2669.

41 Andonegui G, Bonder CS, Green F, *et al.* Endothelium-derived Toll-like receptor-4 is the key molecule in LPS-induced neutrophil sequestration into lungs. *J Clin Invest* 2003; 111: 1011–1020.

42 Zimmerman GA, McIntyre TM, Mehra M, Prescott SM. Endothelial cell-associated platelet-activating factor: a novel mechanism for signaling intercellular adhesion. *J Cell Biol* 1990; 110: 529–540.

43 Parker JC, Townsley MI. Evaluation of lung injury in rats and mice. *Am J Physiol Lung Cell Mol Physiol* 2004; 286: L231–L246.

44 Esper AM, Martin GS. Evolution of treatments for patients with acute lung injury. *Expert Opin Investig Drugs* 2005; 14: 633–645.